The Purple to Blue Transition of Bacteriorhodopsin Is Accompanied by a Loss of the Hexagonal Lattice and a Conformational Change†

Maarten P. Heyn,* Christiane Dudda, Harald Otto, Florian Seiff, and Ingrid Wallat
Biophysics Group, Department of Physics, Freie Universität Berlin, Arnimallee 14, D-1000 Berlin 33, FRG
Received May 4, 1989; Revised Manuscript Received July 11, 1989

ABSTRACT: X-ray diffraction measurements show that in contrast to the purple membrane, the bacteriorhodopsin molecules are not organized in a hexagonal lattice in the deionized blue membrane. Addition of Ca^{2+} restores both the purple color and the normal (63 Å) hexagonal protein lattice. In the blue state, the circular dichroism spectrum in the visible has the typical exciton features indicating that a trimeric structure is retained. Time-resolved linear dichroism measurements show that the blue patch rotates in aqueous suspension with a mean correlation time of 11 ms and provide no evidence for rotational mobility of bacteriorhodopsin within the membrane. The circular dichroism spectra of the blue and the Ca^{2+}-regenerated purple state in the far-UV are different, indicating a small change in secondary structure. The thermal stability of the blue membrane is much smaller than that of the purple membrane. At pH 5.0, the irreversible denaturation transition of the blue form has a midpoint at 61 °C. The photocycle of the blue membrane (λ_{ex} 590 nm) has an L intermediate around 540 nm whose decay is slowed down into the millisecond time range (5 ms). Light–dark adaptation in the blue membrane is rapid with an exponential decay time of 38 s at 25 °C. The purple to blue transition apparently involves a conformational change in the protein leading to a change in the aggregation state from a highly ordered and stable hexagonal lattice to a disordered array of thermally more labile trimers. The conformational change is of a subtle nature, with only a minor effect on the secondary structure but with a major effect on the opsin shift and the photocycle. It is suggested that the transition involves an equilibrium between two states which is shifted by a change in the surface pH.

Isolated light-adapted purple membranes at low ionic strength, with an absorption maximum at 568 nm, can be converted into a blue form (605 nm) by a variety of methods (Kimura et al., 1984; Chang et al., 1985). These involve either the lowering of the bulk pH below 3 or the removal of cations. The two blue preparations are therefore called the acid blue and deionized blue forms. The transition is reversible, and the blue membrane can be converted back to the purple form by adding either base or cations. Both acidification and deionization lead to a decrease of the surface pH. In most respects reported so far, the two blue preparations are identical in properties (Smith & Mathies, 1985). The deionized blue form has as an important advantage over the acid blue form that the membranes do not aggregate and can be obtained in a pure form. The photocycle of the acid blue membrane has very little if any of the intermediate M, and it has therefore been suggested that in the blue state bacteriorhodopsin (bR)[1] does not pump protons (Mowery et al., 1979; Drachev et al., 1978).

It is still an open question whether the transition is brought about by a lowering of the surface pH or by the protonation of a carboxyl group near the chromophore (Fischer & Oesterhelt, 1979). Addition of lipophilic anions (Kamo et al., 1987) or the application of an electric field (Tsuji & Hess, 1986) also lead to the blue form. Further interest in the properties of the blue membrane was generated by the observation that a number of mutants of bR are distinctly "blue" depending on pH (Mogi et al., 1988). For the mutant Asp85-Glu in lauryl maltoside, for instance, the pK of the blue to purple transition is shifted to 8.5, and the blue form has its absorption maximum at 609 nm (Mogi and Khorana, private communication). Similar observations were made with this mutant in purple membrane patches (Butt et al., 1989).

Up to now it has been assumed that the deionized blue membrane has the same hexagonal lattice as the purple membrane (Kimura et al., 1984; Katre et al., 1986). We have investigated the possibility that structural changes between the two forms may be responsible for the differences in properties. Using X-ray diffraction, CD[1] spectroscopy, and transient dichroism, we find that the blue membrane no longer has the hexagonal lattice and that the secondary structure is slightly different but that the trimer structure within an integral membrane patch is retained. The purple to blue transition thus involves a conformational change which affects the protein–protein and protein–lipid contacts. The conformational change and the accompanying change in intertrimer interactions may be induced by the change in surface pH and may be of electrostatic origin. The conformational change leads to a considerably reduced thermal stability. Whereas the structure of bR is stable up to 95 °C (Jackson & Sturtevant, 1978), thermal denaturation of the blue membrane already sets in around 60 °C. The surface pH of the deionized blue membrane is expected to be between 1 and 2 in the absence of significant amounts of salt (Szundi & Stoeckenius, 1988). Internal and surface salt bridges may well break under these conditions, explaining the conformational change and concomitant reduced thermal stability. The changes in color and photocycle may be explained by a subtle local change in conformation which alters the position of charged groups of the protein in the chromophore environment. Whether it is

† Supported by the Bundesministerium für Forschung und Technologie (03-BU 1 FUB) and by the Deutsche Forschungsgemeinschaft (Sfb 312 TP B1).

[1] Abbreviations: bR, bacteriorhodopsin; CD, circular dichroism; UV, ultraviolet.

0006-2960/89/0428-9166$01.50/0

induced by a change in surface pH or by a direct interaction remains to be seen.

Materials and Methods

Preparation of Blue Membranes. Blue membranes were prepared as described (Kimura et al., 1984), by passing purple membranes from strain ET 1001 through an ion-exchange column (Bio-Rad, AG 5W - X4) which had been equilibrated by washing alternately with 1 M HCl and 1 M NaOH. Before addition of the purple membranes, the equilibrated column had a pH of 5.6. The blue membrane suspensions coming off the column had a pH typically of 4.2. Dilutions of the blue membrane were performed with plastic pipets and with deionized Milli-Q water of resistance larger than 18 MΩ·cm. Blue membranes were always handled in plastic ware or quartz containers.

X-ray Diffraction. Freshly prepared blue membranes were diluted with Milli-Q water of pH 5.6 and pelleted by centrifugation in new plastic tubes which had been soaking in deionized water for several days. A concentrated drop of blue membrane pellet was transferred with a plastic pipet to a 10-μm-thick mylar film and allowed to dry at 90% relative humidity. The mylar support with the oriented blue membrane films was mounted in a controlled humidity chamber and formed one window of the chamber. After the support was mounted, the sample was allowed to equilibrate for several hours at 100% relative humidity. The mosaic spread of the oriented stacks of blue membranes was typically 10° (full width at half-height). Absorption measurements of the mylar-supported films taken after conclusion of the X-ray experiments at the transparent edge of the film showed that the samples were still blue. For each experiment, approximately 1 mg of blue membrane was used. The X-ray source was a rotating anode generator (Marconi Avionics GX 21) operating at 35 kV and 55 mA. The Ni-filtered copper K_α radiation of wavelength 1.542 Å was collimated with a collimator of 0.2-mm diameter. To reduce air scattering, the space between sample and film was occupied by a helium-filled chamber. The sample–film distance was typically 15.4 cm and was determined with an accuracy of 0.1 cm. The diffraction data were collected on film (Agfa-Gevaert Osray 3M). Exposure times were typically 25 h. The powder patterns were scanned in steps of 100 μm using a digital densitometer (Optronics). The digitized data were circularly averaged on a VAX computer.

CD Measurements. CD spectra were recorded with a Jasco J-500A spectropolarimeter in cells of 1-cm path length.

Photocycle and Transient Linear Dichroism Measurements. The photocycle was measured with a homemade flash photolysis spectrometer. Excitation was by a 30-mJ XeCl excimer laser (EMG 50, Lambda Physik) which pumped a broad-band dye laser (rhodamine 6G, 590 nm). The pulse length was 10 ns. The energy per flash was between 2 and 3 mJ. Flash-induced transmission changes were detected with the measuring beam crossing the actinic beam at 90° at the sample. An Iwatsu DM 901 transient recorder with a logarithmic time base (8 blocks of 512 points) was used for data acquisition from 0.1 μs to 2s. For photocycle measurements, the polarizer in the measuring beam was set at the magic angle. The kinetics of light–dark adaptation were measured with the same flash spectrometer at 650 nm, in the steepest part of the adsorption spectrum. For these measurements, the cuvette was preilluminated for 60 s with a Schott KL 150 B lamp with a 520-nm cutoff filter and for 5 s under the same conditions before each flash. The kinetics of the absorption change in the second time range due to light–dark adaptation were the same with the actinic flash blocked off or not. For these slow measurements, the time base was set from 1 μs to 100 s. For anisotropy measurements, the data for the two polarizations were recorded sequentially. The light intensity of each flash was monitored with a photodiode and a sample-and-hold-circuit to correct for fluctuations in the laser intensity. Transient linear dichroism experiments were performed as described (Heyn et al., 1977). The time-resolved anisotropy, $r(t)$, was calculated from the measured absorbance changes with polarization parallel ($\Delta A_\parallel$) and perpendicular ($\Delta A_\perp$) to the polarization of the excitation flash as

$$r(t) = \frac{\Delta A_\parallel - \Delta A_\perp}{\Delta A_\parallel + 2\Delta A_\perp} \quad (1)$$

Performance of the instrument was routinely checked with an isotropic sample consisting of gel of immobilized purple membrane. Values of $r(0)$ of 0.38 were obtained for the depletion signal (568 nm). The absorbance data were fitted with a sum of exponentials. The anisotropy data were fitted with a power law corresponding to a distribution of exponentials:

$$r(t) = r(0)(1 + t/n\tau)^{-n} \quad (2)$$

Results

X-ray Diffraction. Figure 1A shows the X-ray diffraction pattern of the blue membrane. Apart from one ring at small angles, only a broad featureless diffraction is observed. The two broad outer rings are due to the mylar windows and support. The pattern in Figure 1B was obtained from the same blue membrane preparation after regeneration with two Ca^{2+} per bR and shows the familiar pattern of the purple membrane. The circularly averaged densitometer tracings corresponding to Figure 1A,B are presented in (A) and (C) of Figure 2. Three reflections due to the hexagonal lattice in (C) are labeled with the corresponding indices (h,k). In panel B, the background due to the system with a clean mylar support, measured under otherwise identical operating conditions, was subtracted and the difference pattern expanded by a factor of 4.4. The horizontal coordinate in Figure 2 is $s = 2 \sin \theta/\lambda$ with θ half the scattering angle. When the reflections of Figure 2C are indexed on a hexagonal lattice, a unit-cell dimension of 62.7 Å is obtained, within experimental accuracy equal to that of the native purple membrane. From Figure 2A, it is clear that the blue membrane does not have a lattice. In the expanded and background-corrected view of Figure 2B, one peak is observed around $s = 0.033$ Å^{-1}, which is close to the position of the (1,1) reflection, and several broad lines and shoulders at 0.037, 0.05, 0.068, 0.088, and 0.115 Å^{-1} which are superimposed on a broad structureless continuous background with a maximum near 0.1 Å^{-1}. These features are close to the expected positions for the (2,0), (2,1), (3,1), (4,1), and (4,3) reflections and are probably due to a small amount of residual purple membrane. This is supported by photocycle experiments (see below) which indicate a small absorbance increase at 410 nm which may be due to the M intermediate of the purple membrane. Similar observations have been made in previous photocycle experiments on blue membranes (Ariki & Lanyi, 1986; Corcoran et al., 1987). The very broad diffraction with a maximum around 0.10 Å^{-1} is most likely due to the interhelix interferences within one bR monomer (average distance around 10 Å) and is known as the monomer peak (Hiraki et al., 1981; Kataoka & Ueki, 1980). Alternative explanations for the superimposed sharper lines and shoulders will be considered under Discussion. In most of our experiments, hydrated oriented multilayers at 100% relative humidity were used. X-ray experiments with aqueous pellets in quartz

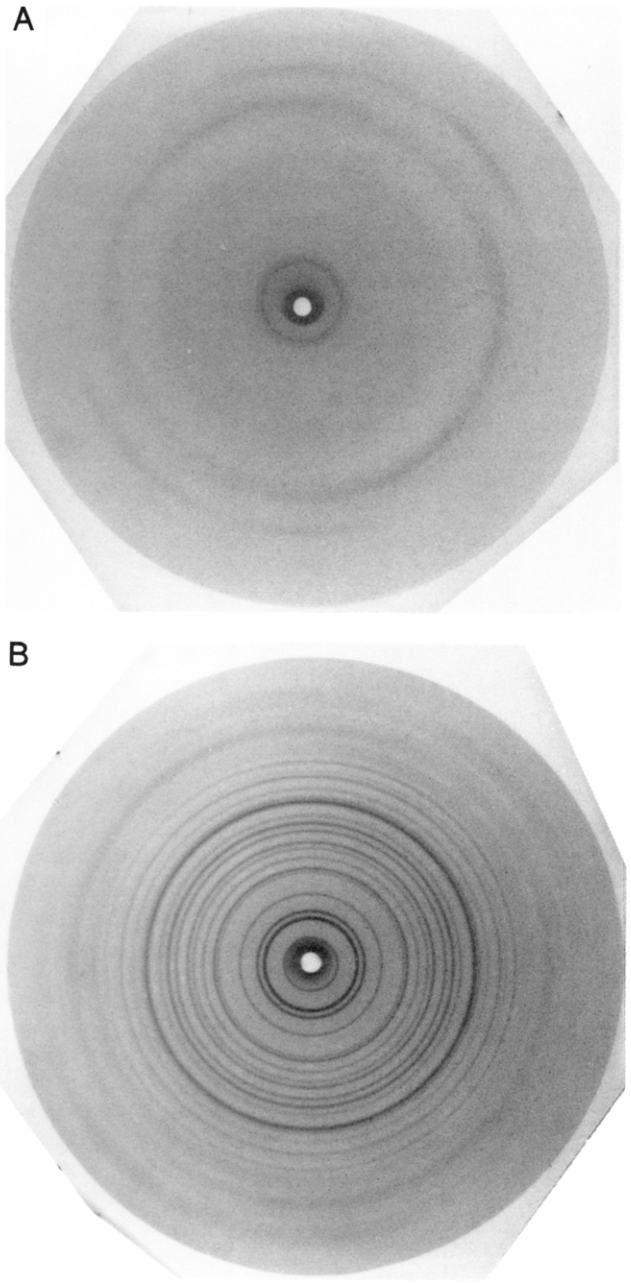

FIGURE 1: X-ray diffraction patterns of oriented multilayers of deionized blue membranes (A) and of blue membranes regenerated with calcium acetate at a molar Ca^{2+} to bR ratio of 2 (B). Sample to film distances: 15.4 cm (A), 17.7 cm (B). Exposure times: 25.5 h (A), 15.0 h (B). Relative humidity: 90%. The incident X-ray beam was perpendicular to the plane of the membranes.

capillaries showed in principle the same results, but due to the lower concentration of membranes, the signal to noise ratio was of poorer quality.

CD Measurements. A 1-cm quartz CD cuvette, which had been exhaustively washed with deionized water, was filled with a dilute solution of blue membrane (0.19 μM, pH 5.3). The CD cuvette was mounted in a Shimadzu UV240 spectrometer, and the absorption spectrum was measured to check that the sample was still in the blue state (data not shown). After measurement of the CD spectrum from 260 to 200 nm, the blue membrane was converted into the purple form by adding between 3 and 10 μL of 2 mM calcium acetate directly into the CD cuvette with a plastic pipet (final Ca/bR ratio between 13 and 43), without significantly diluting the sample (cell volume 2.6 mL). After the CD spectrum of this regenerated sample was measured, the CD cuvette was mounted again in

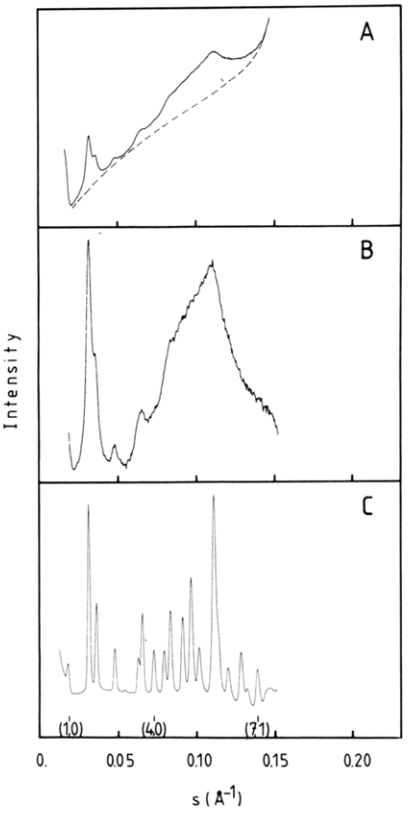

FIGURE 2: Circularly averaged densitometer traces of the X-ray diffraction pictures of Figure 1. The intensities are plotted versus $s = 2 \sin \theta/\lambda$. θ is half the scattering angle. (A) Densitogram for the blue membrane. The dashed line is the observed system background (exposure time 25.5 h). (B) The data of (A) after subtraction of the background and expansion by a factor of 4.4. (C) Densitogram of the blue membrane after regeneration with two Ca^{2+} per bR. Of the diffraction peaks expected for a hexagonal lattice of unit-cell dimension 62.7 Å, three are labeled with the (h,k) indices (1,0), (4,0), and (7,1).

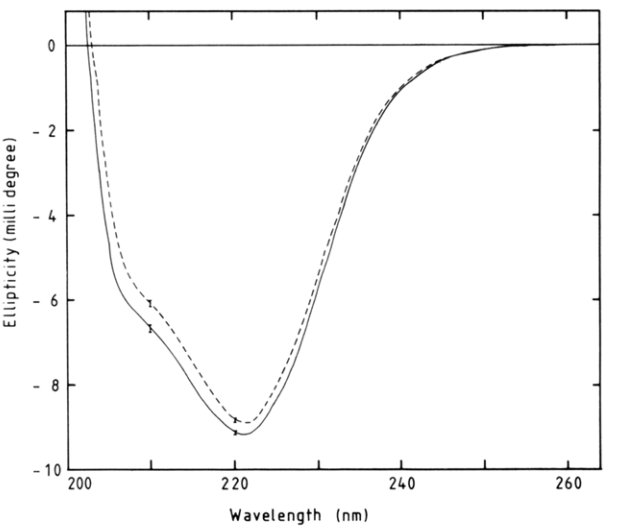

FIGURE 3: Far-UV circular dichroism spectra of the deionized blue membrane (—) and the Ca^{2+}-regenerated blue membrane (---). Conditions: bR concentration 0.19 μM, pH 5.3, molar Ca^{2+} to bR ratio 13, temperature 25 °C, dark-adapted. Each trace is the average of 16 spectra. Four independent sets of experiments were performed. The error bars at 210 and 220 nm are measures of the noise and the reproducibility of the data.

the Shimadzu spectrometer, and its absorption spectrum was recorded to show that its maximum had returned to 568 nm. The two CD spectra are shown in Figure 3. The concentration and path length were chosen to get optimal signal to noise and

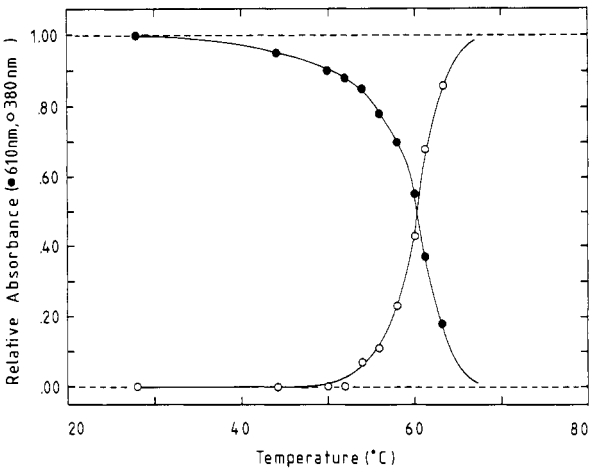

FIGURE 4: Thermal denaturation of the deionized blue membrane. The normalized relative absorbance changes at wavelength 610 nm (●) and 380 nm (○) are plotted versus the temperature, $[A(T) - A(25)]/[A(\infty) - A(25)]$, at 380 nm and, $[A(T) - A(\infty)]/[A(25) - A(\infty)]$, at 610 nm; $A(T)$ is the absorbance at the temperature T (degrees centigrade). The temperature was measured inside the cuvette, pH 5.0.

maximal amplitude on the 0.5 mdeg/cm scale. There is a small but significant difference between the two spectra. The amplitude of the CD spectrum of the blue form at 220 and 210 nm is 3% and 10%, respectively, larger than in the purple form. The acid blue membrane at low pH is highly aggregated, and it is thus very difficult to make a bona fide comparison with the CD spectrum of the purple membrane, due to the differences in light-scattering and absorption flattening artifacts in the two samples (Heyn, 1989). These problems are absent in the present case. In the CD spectrum around 605 nm, the characteristic exciton bands were observed (data not shown), indicating that the bR molecules are not in the monomeric state (Heyn et al., 1975; Heyn, 1989).

Thermal Stability. The absorption spectra of blue membranes were recorded as a function of temperature in a Shimadzu 240 spectrometer with a thermostatable cuvette holder. The temperature was measured inside the stoppered cuvette with a thermocouple. The temperature was changed with a Julabo F20 thermostat. The relative absorbance at 610 and 380 nm is plotted as a function of temperature in Figure 4. For temperatures above 55 °C, a steep drop in the absorbance at 610 nm occurs which is irreversible. The highest temperature points are thus not meaningful, since the thermodynamic equilibrium was not reached. Concomitantly with the decrease at 610 nm, the absorbance at 380 nm increases, indicating the denaturation of bacteriorhodopsin with loss of the chromophore. The stability depends critically on the pH, increasing with increasing pH [see also Cladera et al., (1988)]. The irreversible destruction of the retinal–opsin complex is not accompanied by a major unfolding of the protein. The thermal transition of the blue membrane was also monitored by CD measurements in the far-UV (data not shown). Between 25 and 75 °C, the CD amplitude at 220 nm decreases by only about 30%. This is close to the corresponding value for the purple membrane (Brouilette et al., 1987).

Photocycle and Anisotropy Measurements. Photocycle data were collected at 16 wavelengths varying from 390 to 690 nm in steps of 20 nm. The projection of the surface of absorbance changes, $\Delta A(\lambda,t)$ onto the (λ,t) plant is shown in Figure 5. The points of constant ΔA are plotted as contour lines. In Figure 5A,B, the photocycles of the blue and purple membranes are compared in the time range from microseconds to seconds. Excitation was at 590 nm. In this presentation, the

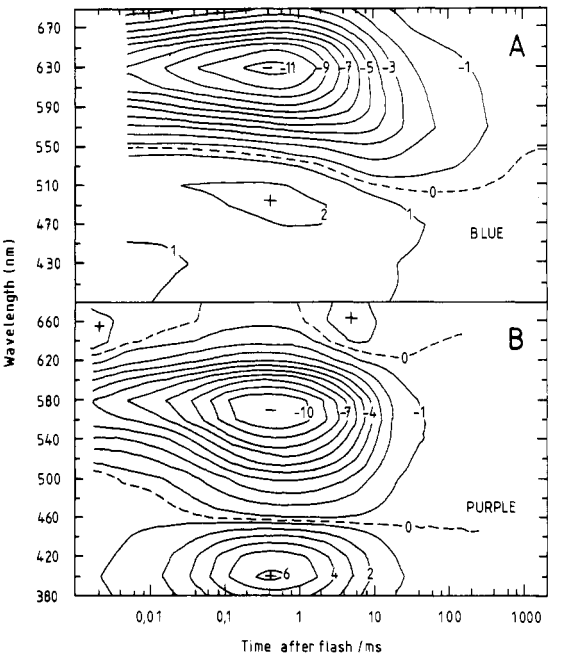

FIGURE 5: Comparison of the photocycles of the deionized blue (A) and the purple membrane (B). Lines of equal absorbance change are plotted in the (λ,t) plane and are labeled with the corresponding ΔA values (arbitrary units). Maxima and minima in ΔA are labeled with + and −, respectively. For each sample, the photocycle was measured at 16 wavelengths. Conditions: 25 °C, dark-adapted, λ_{ex} = 590 nm, pH 4.2.

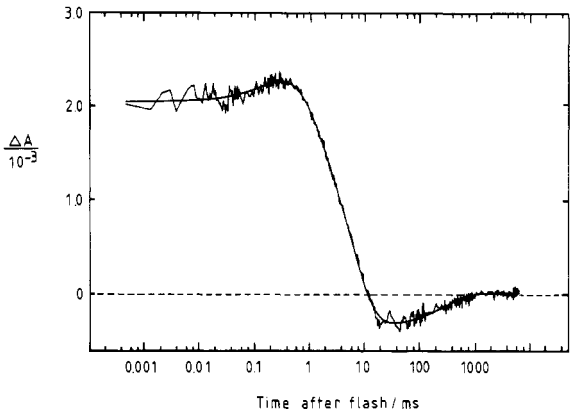

FIGURE 6: Photocycle of the deionized blue membrane at 510 nm. The data were fitted with a sum of exponentials. The main decay component has a relaxation time of 5.5 ms. The negative absorbance change decays with a time of 290 ms.

differences are particularly striking. The negative depletion signal occurs at 630 nm in the blue membrane, as compared to 570 nm in the purple membrane. In comparison with the purple membrane, the line of zero absorbance change occurs at a much higher wavelength in the blue membrane. In the blue form, there is very little absorbance change near 410 nm where one normally observes the M intermediate. Instead, a rather flat, small positive absorbance change occurs with a maximum between 500 and 510 nm. In Figure 6, the data at 510 nm are shown. For the purple membrane, the absorption change at this wavelength is negative for all times. One advantage of the logarithmic presentation of Figure 6 is that the decay times of exponential processes occur at the inflection points of the curve. The positive absorbance change at this wavelength thus decays with a time constant of 5.5 ms. The amplitude spectrum of this millisecond component, obtained by a global analysis of the absorbance changes at all 16 wavelengths, has its positive maximum around 540 nm.

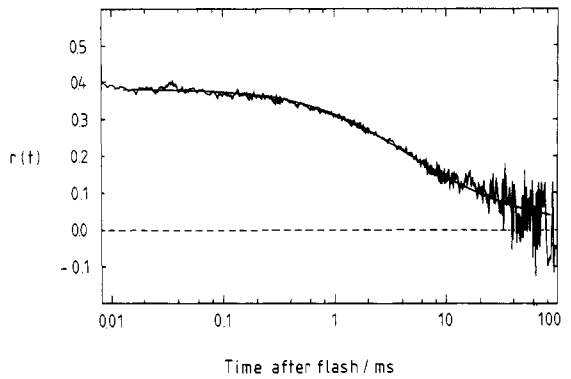

FIGURE 7: Decay of the transient dichroism of the depletion signal of the deionized blue membrane at 620 nm (excitation at 590 nm). The initial anisotropy is 0.382. The continuous curve is a fit with a single-power law with $n = 0.65$ and $\tau = 4.39$ ms. The mean decay time is 11.3 ms.

Due to the overlap of several components in this wavelength region, the amplitude is reduced and the apparent maximum shifted to 510 nm. The slow component in the decay of the absorbance change with a time constant of about 300 ms is apparent. This component is also observed at other wavelengths (see Figure 5a). There is furthermore no O intermediate in the blue form.

The kinetics of light–dark adaptation were monitored at 650 nm (data not shown). The absorbance change was negative with an approximately exponential decay with a time constant of 38 s at 25 °C. This shows that the dark-adapted state has a smaller absorbance at this wavelength and that the kinetics of dark adaptation are at least an order of magnitude faster than in the purple membrane under the same conditions. The photocycle data reported above and summarized in Figure 5A were recorded without preillumination before each flash and thus refer to the dark-adapted state containing a 1:1 mixture of 13-cis and all-trans isomers (Mathew et al., 1986). Repeating the photocycle measurements with 5-s preillumination before each flash, as described for the light–dark adaptation experiments, increases the relative contribution of the all-trans isomer to the photocycle (Mathew et al., 1986). Light-adapting before each flash did not significantly change the kinetics of the cycle, however, but increased the amplitudes. It is thus likely that we are observing the kinetics of the all-trans photocycle.

The anisotropy of the depletion signal at 620 nm is plotted versus log time in Figure 7. The anisotropy remains initially constant at a value of 0.38, close to the theoretical limit of 0.4, and decays with a mean decay time of about 11 ms. The noise increases of course with increasing time since the absorbance changes go to zero. We conclude that the blue patches rotate with a characteristic time which is close to that observed for purple membrane patches and that no rotational motion of bacteriorhodopsin occurs within the patch on the time scale from microseconds to milliseconds.

Discussion

Two lines of evidence suggest that the purple membrane should be considered as a lattice of bacteriorhodopsin trimers and that the trimer is the basic building block. First of all, differential scanning calorimetry, X-ray diffraction, and CD experiments show that around 80 °C a reversible transition occurs in the purple membrane from a hexagonal protein lattice to a disordered array of trimers (Jackson & Sturtevant, 1978; Hiraki et al., 1981). On the basis of extensive model calculations, the X-ray diffraction pattern which remained above the transition was interpreted as the sum of a broad continuous contribution due to interhelical interferences from the monomer (0.1 $Å^{-1}$) and of superimposed modulations due to intratrimer interferences (Hiraki et al., 1981; Kataoka & Ueki, 1980). In agreement with this interpretation, the visible CD spectra above 80 °C still had the exciton features (Hiraki et al., 1981). The calorimetry data demonstrated that the transition was highly cooperative, as expected for a crystallization process (Jackson & Sturtevant, 1978). In the second place, partial delipidation of the purple membrane leads to a change in lipid–protein and protein–protein contacts and to a contracted lattice of reduced unit-cell dimensions (Henderson et al., 1982; Glaeser et al., 1985; Tsygannik & Baldwin, 1987). The trimer structure is retained, however, in the lipid-depleted membrane without a change in the structure of the monomer (Tsygannik & Baldwin, 1987).

The X-ray diffraction pattern observed for the blue membrane (Figures 1 and 2) is similar to that of the purple membrane above the 80 °C transition and may likewise be interpreted as being due to disordered trimers. In support of this interpretation, the visible CD spectra are of the exciton type. Recent microcalorimetric experiments demonstrated that in the blue membrane the equivalent of the 80 °C transition of purple membrane is absent and that it is reestablished only after regeneration with at least two Ca^{2+} per bR (Cladera et al., 1988). On the basis of the present X-ray diffraction results, these observations may be explained in a very simple way. Since the blue membrane has no lattice, no order–disorder transition can be observed in the temperature dependence of the specific heat. Addition of two Ca^{2+} per bR regenerates the lattice and leads to the reappearance of the transition.

Although no X-ray diffraction data have been published for the blue membrane, contradictory descriptions have appeared claiming a "well-preserved lattice" for the deionized blue form (Kimura et al., 1984) and "no lattice structure" for the acid blue form (Mowery et al., 1979). Since the two forms of the blue membrane are indistinguishable in many respects and are generally considered to be identical, it seems unlikely that such a discrepancy would exist. The deionized blue form is an excellent cation indicator with an effective dissociation constant for di- and trivalent cations in the micromolar range (Ariki & Lanyi, 1986). It is thus possible that the report of the lattice (Kimura et al., 1984) is due to partial regeneration by contaminating cations. In itself, the lack of a lattice is not unusual. The lattice is absent in the apomembrane, in the white membrane of retinal-minus mutants, in some chemically modified purple membranes, in purple membranes regenerated with certain retinal analogues, and in some mutants of bR. The few remaining weak features in the X-ray diffraction pattern of the blue membrane may be interpreted as being due to trimers as argued above. Alternatively, these broad lines may be due to small areas of residual purple membrane. The transition to the blue state may not be complete. In the X-ray diffraction pattern, we observe after all only the diffracting material. Even a few percent crystalline purple membrane will be detected. This interpretation is in accordance with the small positive absorbance change at 410 nm which may be due to the M intermediate of the purple membrane. A third explanation is that in the disordered blue patch the bR molecules remain close to their original positions in the hexagonal lattice with rotational disorder of trimers, leading to diffuse diffraction.

Small but reproducible changes were observed in the far-UV CD spectrum, indicating a minor change in secondary structure. The two spectra of Figure 3 were at the same pH (5.3). At the low concentration of bR used in the measurements (0.19

μM), the pH does not drop upon addition of cations to the blue membrane. Absorption measurements in the wavelength range from 250 to 700 nm showed that the light scattering did not change when Ca^{2+} was added. Light-scattering artifacts may easily distort the CD spectra of membrane proteins (Heyn, 1989). If the amount of light scattering does not change in a transition, however, it is correct to interpret the difference in the CD spectra as evidence for a conformational change.

The photocycle of the blue membrane has been investigated before (Mowery et al., 1979; Kobayashi et al., 1983; Ohtani et al., 1986; Chronister et al., 1986). In these reports as well as in others (Ariki & Lanyi, 1986; Corcoran et al., 1987), the absorbance change at 410 nm is typically about 10% of that of the purple membrane and may be due to the M intermediate of a residual amount of purple membrane. Either the 100% blue state has never been reached or this positive absorbance change at 410 nm is part of the blue cycle. Typical for the blue state is a shallow positive absorbance change with peak between 500 and 510 nm which decays in 5 ms. The amplitude spectrum of this millisecond component has its maximum at 540 nm, suggesting that it is an L-type intermediate. This interpretation is in accordance with previous resonance Raman (Chronister et al., 1986) and photocycle (Kobayashi et al., 1983) experiments. The decay of this L analogue is slowed down into the millisecond range, the deprotonation of the Schiff base and the formation of M are inhibited, presumably since the proton acceptor is already protonated. The very slow components in the return to the ground state remain to be explained. The rapid light–dark adaptation, which is at least an order of magnitude faster than in the purple membrane, also provides evidence for a difference in the protein–chromophore contacts between the blue and purple states. The high initial anisotropy $r(0)$ means that little or no rotation occurred for times less than 8 μs. In the accessible time interval, no rapid rotational motion was observed either, and the slow millisecond decay is due to the rotation of the blue membranes. It is reasonable that no rotational mobility due to monomers or trimers occurs, since in the disordered state the mean protein–protein distances remain the same as in the lattice and the effective viscosity due to the dense packing will be very high.

It has been suggested previously, mainly on the basis of spectroscopic measurements, that a conformational change occurs during the transition from the deionized blue to the purple membrane. Most of these arguments are indirect or inconclusive. Changes in the near-UV CD spectra (Kimura et al., 1984) and in the tryptophan emission (Jang et al., 1988; Mercier et al., 1988) cannot be unambiguously attributed to changes in conformation since a large change in chromophore absorption occurs as well. For the case of the near-UV CD spectra of the acid blue membrane (Muccio & Cassim, 1979), the changes were entirely attributed to the changes in the chromophore spectrum and to the resulting change in tryptophan–chromophore coupling. The observed increase in the tryptophan fluorescence (Jang et al., 1988; Mercier et al., 1988) in going from purple to blue may likewise be simply due to the decreased spectral overlap between tryptophan and the chromophore, leading to a reduction in energy transfer. The difference absorption spectra in the near-UV provide some evidence for a more polar environment of some tryptophans in the blue state (Dunach et al., 1988). Kinetic experiments on the blue to purple transition using the stopped-flow method indicate the presence of at least three components with relaxation times which are slow enough for a conformational change (Fischer & Oesterhelt, 1979; Zubov et al., 1986; Kimura et al., 1984). The relaxation time of one of the components was independent of the cation concentration, consistent with an intramolecular isomerization such as a conformational change or light–dark adaptation (Zubov et al., 1986). The absence of an isosbestic point in the absorption spectrum for the blue to purple transition also indicates that it is not a simple two-state equilibrium but may involve a conformational change.

The experimental results and their interpretation may be summarized as follows. The diffraction results show that the hexagonal protein lattice is absent in the blue membrane and that addition of two Ca^{2+} per bR restores both the purple color and the two-dimensional crystalline structure. In agreement with previous work (Kimura et al., 1984), the CD spectra of the blue form in the visible have the characteristic exciton features indicating some form of protein aggregation, most likely the trimer. The transient dichroism data suggest that the bR molecules do not rotate within the membrane and that the depolarization is due to the rotation of whole blue membranes. The CD spectra of the protein backbone reveal minor differences in secondary structure between the blue and purple states consistent with a small conformational change. The thermal denaturation experiment demonstrates that the blue form has a markedly reduced thermal stability in comparison with the purple membrane. In the blue state, which has a very low surface pH, possibly some salt bridges near the membrane surface which stabilize the native structure are broken. Taken together, these measurements show that in the blue membrane the bR molecules are arranged in a state without long-range order but with small aggregates which lack rotational mobility. A small conformational change of the protein induces this change in aggregation. In the neighborhood of the chromophore, already minor changes in the distances of counterions and charges are sufficient to cause a large wavelength shift in the absorption spectrum and a major change in the photochemical cycle.

Alternative explanations which invoke a specific protonation change cannot be excluded. The lowering of the surface pH could, for instance, lead to the protonation of an internal carboxyl group close to the chromophore. With this group protonated, the pigment is blue, and the protein is in a different conformation. If this carboxyl also serves as the acceptor of the Schiff base proton, its protonation in the blue membrane could in addition explain why formation of the M intermediate is inhibited. Of the four internal aspartic acid residues of bR, both Asp85 and Asp212 are candidates of such a role. It is of interest that mutants at both of these positions exist which are deficient in proton pumping and have a blue pigment (Mogi et al., 1988; Mogi, Marti, and Khorana, private communication; Butt et al., 1989). Further work on these mutants may well provide new insights into the mechanism of the purple to blue transition.

Acknowledgments

We thank Prof. Walther Stoeckenius for critical comments and suggestions.

References

Ariki, M., & Lanyi, J. K. (1986) *J. Biol. Chem. 261*, 8167–8174.

Brouillette, C. G., Muccio, D. D., & Finney, T. K. (1987) *Biochemistry 26*, 7431–7438.

Butt, H. J., Fendler, K., Bamberg, E., Tittor, J., & Oesterhelt, D. (1989) *EMBO J. 8*, 1657–1663.

Chang, C.-H., Chen, J.-G., Govindjee, R., & Ebrey, T. (1985) *Proc. Natl. Acad. Sci. U.S.A. 82*, 396–400.

Chronister, E. L., Corcoran, T. C., Song, L., & El-Sayed, M. A. (1986) *Proc. Natl. Acad. Sci. U.S.A. 83*, 8580-8584.
Cladera, J., Galisteo, M. L., Dunach, M., Mateo, P. L., & Padros, E. (1988) *Biochim. Biophys. Acta 943*, 148-156.
Corcoran, T. C., Ismail, K. Z., & El-Sayed, M. A. (1987) *Proc. Natl. Acad. Sci. U.S.A. 84*, 4094-4098.
Drachev, L. A., Kaulen, A. D., & Skulachev, V. P. (1978) *FEBS Lett. 87*, 161-167.
Dunach, M., Padros, E., Seigneuret, M., & Rigaud, J.-L. (1988) *J. Biol. Chem. 263*, 7555-7559.
Fischer, U., & Oesterhelt, D. (1979) *Biophys. J. 28*, 211-230.
Glaeser, R. M., Jubb, J. S., & Henderson, R. (1985) *Biophys. J. 48*, 775-780.
Henderson, R., Jubb, J. S., & Rossmann, M. G. (1982) *J. Mol. Biol. 154*, 501-514.
Heyn, M. P. (1989) *Methods Enzymol. 172*, 575-584.
Heyn, M. P., Bauer, P.-J., & Dencher, N. A. (1975) *Biochem. Biophys. Res. Commun. 67*, 897-903.
Heyn, M. P., Cherry, R. J., & Müller, U. (1977) *J. Mol. Biol. 117*, 607-620.
Heyn, M. P., Cherry, R. J., & Dencher, N. A. (1981) *Biochemistry 20*, 840-849.
Hiraki, K., Hamanaka, T., Mitsui, T., & Kito, Y. (1981) *Biochim. Biophys. Acta 647*, 18-28.
Jackson, M. B., & Sturtevant, J. M. (1978) *Biochemistry 17*, 911-915.
Jang, D.-J., Corcoran, T. C., & El-Sayed, M. A. (1988) *Photochem. Photobiol. 48*, 209-217.
Kamo, N., Yoshimoto, M., Kobatake, Y., & Itoh, S. (1987) *Biochim. Biophys. Acta 904*, 179-186.
Kataoka, M., & Ueki, T. (1980) *Acta Crystallogr. A36*, 282-287.
Katre, N. V., Kimura, Y., & Stroud, R. M. (1986) *Biophys. J. 50*, 277-284.
Kimura, Y., Ikegami, A., & Stoeckenius, W. (1984) *Photochem. Photobiol. 40*, 641-646.
Kobayashi, T., Ohtami, H., Iwai, J., Ikegami, A., & Uchiki, H. (1983) *FEBS Lett. 162*, 197-200.
Mathew, M. K., Scherrer, P., & Stoeckenius, W. (1986) *Biophys. J. 49*, 211a.
Mercier, G., & Dupuis, P. (1988) *Photochem. Photobiol. 47*, 433-438.
Mogi, T., Stern, L. J., Marti, T., Chao, B. H., & Khorana, H.-G. (1988) *Proc. Natl. Acad. Sci. U.S.A. 85*, 4148-4152.
Mowery, P. C., Lozier, R. H., Quae, C., Tseng, Y.-W., Taylor, M., & Stoeckenius, W. (1979) *Biochemistry 18*, 4100-4107.
Muccio, D. D., & Cassim, J. Y. (1979) *J. Mol. Biol. 135*, 595-609.
Ohtani, H., Kobayashi, T., Iwai, J., & Ikegami, A. (1986) *Biochemistry 25*, 3356-3363.
Smith, S. O., & Mathies, R. A. (1985) *Biophys. J. 47*, 251-254.
Szundi, I., & Stoeckenius, W. (1987) *Proc. Natl. Acad. Sci. U.S.A. 84*, 3681-3684.
Szundi, I., & Stoeckenius, W. (1988) *Biophys. J. 54*, 227-232.
Tsuji, K., & Hess, B. (1986) *Eur. Biophys. J. 13*, 273-280.
Tsygannik, I. N., & Baldwin, J. M. (1987) *Eur. Biophys. J. 14*, 263-272.
Zubov, B. K., Tsuji, K., & Hess, B. (1986) *FEBS Lett. 200*, 226-230.

General Mechanism for the Bacterial Toxicity of Hypochlorous Acid: Abolition of ATP Production†

William C. Barrette, Jr.,‡ Diane M. Hannum, William D. Wheeler,§ and James K. Hurst*
Department of Chemical and Biological Sciences, Oregon Graduate Center, Beaverton, Oregon 97006-1999
Received April 25, 1989; Revised Manuscript Received July 10, 1989

ABSTRACT: The adenylate energy charges (EC) of *Escherichia coli* 25922, *Pseudomonas aeruginosa* 27853, and *Streptococcus lactis* 7962 rapidly fell in nutrient-rich media from values in excess of 0.9 to below 0.1 when the organisms were exposed to lethal levels of HOCl. The same cells maintained in energy-depleted states were incapable of attaining normal EC values necessary for biosynthesis and growth when challenged with nutrient energy sources after HOCl exposure. These changes correlated quantitatively with loss of replicative capabilities. Initial rates of transport of glucose, succinate, and various amino acids that act as respiratory substrates and the ATP hydrolase activity of the F_1 complex from the ATP synthase of *E. coli* 25922 also declined in parallel with or preceded loss of viability. These results establish that cellular death is accompanied by complete disruption of bacterial ATP production by both oxidative and fermentative pathways as a consequence of inhibition of inner membrane bound systems responsible for these processes.

The potent microbicide hypochlorous acid (HOCl) is generated in activated neutrophils by myeloperoxidase (MPO)[1]-catalyzed peroxidation of chloride ion (Klebanoff, 1988; Hurst & Barrette, 1989). The role of HOCl in the bactericidal action of the blood leukocytes has been extensively discussed in relation to other putative toxins (Klebanoff, 1988; Hurst & Barrette, 1989; Elsbach & Weiss, 1983; Spitznagel, 1984; Ganz et al., 1985). Molecular mechanisms of killing by these various toxins have not yet been elucidated, so it has not been possible to assign a primary role to any one of them. Nonetheless, HOCl is toxic to virtually all cell types (Klebanoff & Clark, 1978), its detection in normal stimulated neutrophils

† This work was supported by Public Health Service Grant AI-15834 from the National Institute of Allergy and Infectious Diseases.
* Author to whom correspondence should be addressed.
‡ Present address: BIOSYS, 1057 East Meadow Circle, Palo Alto, CA 94303.
§ Present address: Department of Chemistry, University of Wyoming, Laramie, WY 82071.

[1] Abbreviations: AMG, methyl α-glucopyranoside; CCCP, carbonyl cyanide 3-chlorophenylhydrazone; DTT, dithiothreitol; EC, energy charge; mRNA, messenger RNA; MPO, myeloperoxidase; PBS, phosphate-buffered saline; PMF, proton-motive force.

0006-2960/89/0428-9172$01.50/0